JACS
JOURNAL OF THE AMERICAN CHEMICAL SOCIETY

Communication

pubs.acs.org/JACS

Molecular Ferroelectric with Most Equivalent Polarization Directions Induced by the Plastic Phase Transition

Heng-Yun Ye,* Jia-Zhen Ge, Yuan-Yuan Tang, Peng-Fei Li, Yi Zhang, Yu-Meng You,* and Ren-Gen Xiong*

Ordered Matter Science Research Center, Southeast University, Nanjing 211189, People's Republic of China

Supporting Information

ABSTRACT: Besides the single crystals, ferroelectric materials are actually widely used in the forms of the polycrystals like ceramics. Multiaxial ferroelectrics with multiple equivalent polarization directions are preferable for such applications, because more equivalent ferroelectric axes allow random spontaneous polarization vectors to be oriented along the electric field to achieve a larger polarization after poling. Most of ceramic ferroelectrics like $BaTiO_3$ have equivalent ferroelectric axes no more than three. We herein describe a molecular-ionic ferroelectric with 12 equivalent ferroelectric axes: tetraethylammonium perchlorate, whose number of axes is the most in the known ferroelectrics. Appearance of so many equivalent ferroelectric axes benefits from the plastic phase transition, because the plastic phase usually crystallizes in a highly symmetric cubic system. A perfect macroscopic ferroelectricity can be obtained on the polycrystalline film of this material. This finding opened an avenue constructing multiaxial ferroelectrics for applications as polycrystalline materials.

Ferroelectrics are one of the most studied and utilized polar crystalline materials. The primary feature distinguishing ferroelectrics from other polar pyroelectrics is that the ferroelectric spontaneous polarization can be switched with an applied electric field. As demonstrated by ferroelectric ceramics, most of their applications are based on the polarization switching, such as ferroelectric memory where the $\pm P_r$ (remnant polarization of ferroelectrics) denote "1" and "0" in the binary system, and electro-optic devices where optical properties are controlled by switching polar domains using electric fields. It is worth noting that the spontaneous polarization vector should be along a particular direction (ferroelectric axis) in a ferroelectric single crystal. Therefore, single-crystal ferroelectrics should be well oriented to the ferroelectric axis to achieve the largest polarization. For a uniaxial ferroelectric, the spontaneous polarization vector can be switched between two opposite directions using an electric field, whereas for a multiaxial ferroelectric, it can be switched between multiple directions. Different from single-crystalline ferroelectrics, polycrystalline ferroelectrics like ceramics and spin-coated organic films are the aggregates of single-crystal grains where polarization directions are random. Theoretically, with more equivalent ferroelectric axes exist in a single-crystalline grain, the corresponding polycrystalline sample can achieve a larger polarization after poling and the polarization can be switched more easily. That is why ferroelectric ceramics consisting of multiaxial single-crystal grains, such as $BaTiO_3$ ceramic, can achieve large polarization after poling. Therefore, the number of equivalent ferroelectric axes is an important characteristic for application of polar polycrystalline materials.

Much progress has been made experimentally and theoretically, regarding molecule-based ferroelectrics.[1] Although a pioneer theoretical work has predicted the existing of multistable ferroelectric polarization in molecular ferroelectric compounds,[2] experimental reports of multiaxial molecular ferroelectric are very limited.[3] It has been deduced that the number of the equivalent polarization directions depends on the symmetry change between the high temperature paraelectric phase (PP) and the low temperature ferroelectric phase (FP), i.e., $n = N_p/N_f$, where n is the number of the equivalent polarization directions, N_p is the order of the point group of the PP and N_f is the order of the point group of the FP. In this aspect, plastic phases seem to be the suitable phases for exploring the multiaxial ferroelectricity, because they are characterized by high symmetry (often cubic) and easily transit into stable low symmetric phases. Plastic phases exhibit many unusual properties and have a few interesting potential applications.[4] However, examples of ferroelectrics induced by plastic phase transitions are rare.[3c] In this work, we report a molecular ferroelectric compound with plastic phase transition: tetraethylammonium perchlorate (**1**) (Figure 1). **1** has 12 equivalent ferroelectric axes, which is the most in the known ferroelectrics as far as we are aware.

1 is a commercially available material, and its crystals can be easily grown by slow evaporation of the alcoholic or aqueous solution. The purity of the bulk phase was verified by infrared spectroscopy (IR) and powder X-ray diffraction (PXRD), as shown in Figures S1 and S2, Supporting Information. At room

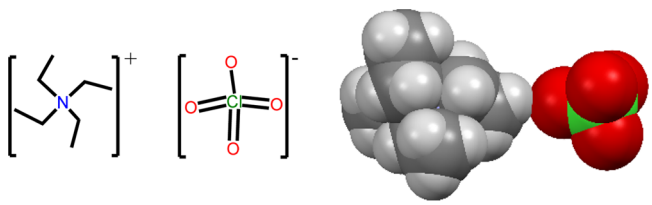

Figure 1. Structural formula and space-filling drawing of **1**.

Received: August 23, 2016
Published: September 28, 2016

DOI: 10.1021/jacs.6b08817
J. Am. Chem. Soc. 2016, 138, 13175−13178

temperature, **1** crystallizes in the polar space group *Cc*.[5] The crystal has a layered structure along the *a*-direction (Figure 2a),

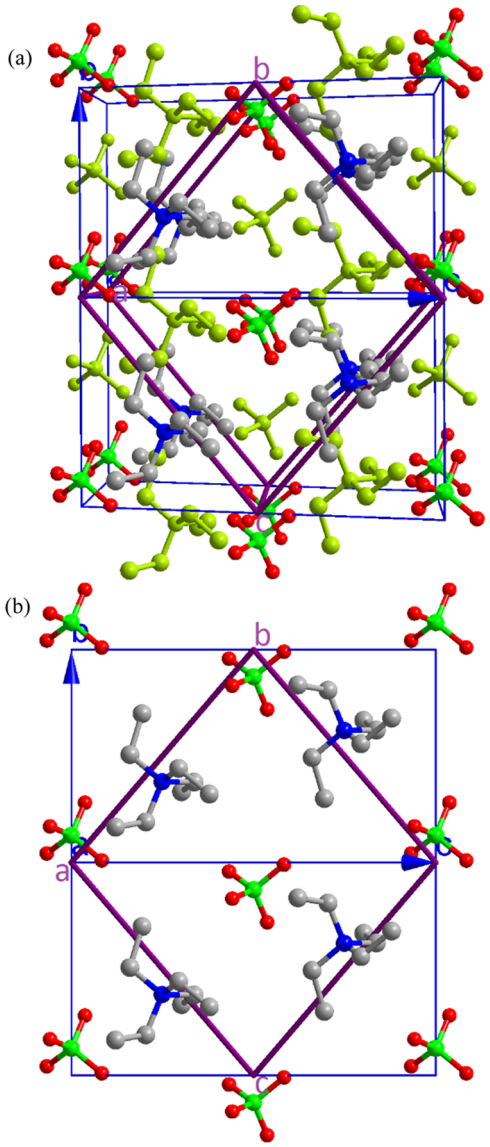

Figure 2. Packing diagrams of the crystal structure of **1**. (a) The perspective view of the crystal structure, showing the layered structure. The molecules were drawn with two-colored bonds and lime bonds respectively to show the two neighbored layers. The cell with purple edge represents the cell from that of the cubic high temperature phase by the lattice twist. (b) The projection of a [1 0 0] layer, showing the similarities to and differences from that of a [1 0 0] layer in NaCl.

and the cations and anions are arranged alternatively along the *b*- and *c*-axes. (Figure 2b and Figure S3 in the Supporting Information). Whether such a polar structure is ferroelectric depends on the existence of a PP at higher temperature.

We then carried out series of temperature dependent studies to characterize the phase-transition properties, as well as the structural information on the high-temperature phase of **1**. By thermal analysis and dielectric measurements (Figure 3a,b), a high temperature phase transition was clearly observed at T_c = ~378 K. Also, at T_c, a transition of second harmonic generation (SHG) signal of zero to a finite intensity reveals a breakdown of centrosymmetry of the high temperature crystal structure. Such a change between the centrosymmetric high temperature phase

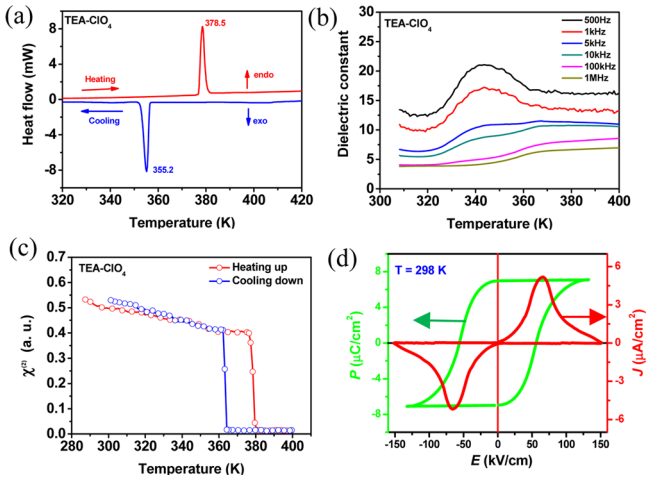

Figure 3. Ferroelectric and related properties for the plastic phase transition of **1**. (a) The DSC curve for **1**. (b) The temperature dependence of the real part of the complex dielectric constant. (c) The temperature dependence of the SHG signal. (d) The field dependence of the spontaneous polarization.

(HTP) and the polar low temperature phase (LTP) indicates that **1** undergoes a potential ferroelectric phase transition.

To test the polarization reversal (ferroelectricity) of the polycrystalline samples, we first tried to measure the polarization−electric field (*P*−*E*) hysteresis loops of the powder-pressed pellets using the traditional Sawyer−Tower circuit. The polarization response is almost linear, showing no polarization-reversal-induced hysteresis. Because the high coercive field usually prevents the switching of polarization, we employed a thin film of **1** to achieve a smaller coercive voltage (for details of thin-film preparation, see the Supporting Information). The as-prepared film shows good crystallinity verified by the PXRD, and the measured area just contains a few grains. Using the double-wave method, which removes the nonhysteresis components from the measurement,[6] we finally obtained the typical ferroelectric *J*−*E* curve and *P*−*E* hysteresis loop at room temperature (Figure 3d). The measured P_s (saturate polarization) is about 7.0 μC/cm^2, which is among the largest in recent emerging molecule-based ferroelectrics.[1a,h,7] The extracted coercive field E_c from the *P*−*E* hysteresis loop is about 70 kV/cm. Such a large coercive field intensity (slightly smaller than that of croconic acid)[8] explains the reason that we can not reverse the polarization on the bulk sample, since it requires a giant bias voltage (>7 kV) on the typical bulk sample with thickness of 1 mm.

The polarization reversal was further investigated using piezoresponse force microscopy (PFM). It can offer non-destructive visualization of ferroelectric domains at the nanometer scale.[9] In the PFM measurement, both the intensities and orientations of the polarizations can be obtained in the form of amplitude and phase. Figure 4 illustrates the lateral PFM phase and amplitude images for the film surface of **1**. It demonstrates two kinds of representative domain structures: stripe-like one (Figure 4a,b), like that in $BiFeO_3$, and rectangle one (Figure 4c,d). The striking phase contrast indicates the oppositely oriented domains separated by domain walls (hatched regions in Figure 4b,d). The domain structures revealed by the amplitude and phase images are consistent. Furthermore, the dependence of phase and amplitude on V_{DC} display a hysteresis loop and a butterfly curve respectively

DOI: 10.1021/jacs.6b08817
J. Am. Chem. Soc. 2016, 138, 13175−13178

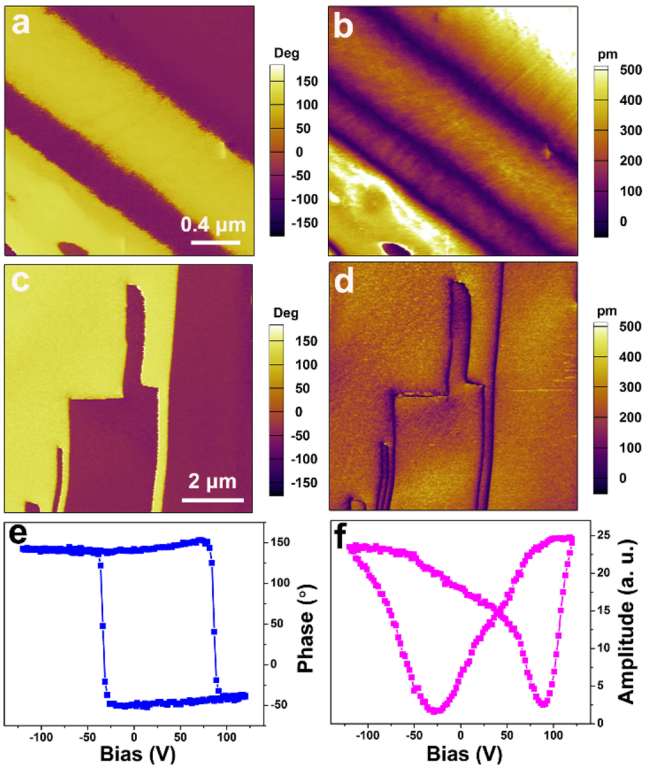

Figure 4. Lateral PFM phase (a, c) and amplitude images (b, d) for the thin film of compound **1**. (e, f) Phase and amplitude signals as functions of the tip voltage for a selected point, showing local PFM hysteresis loops.

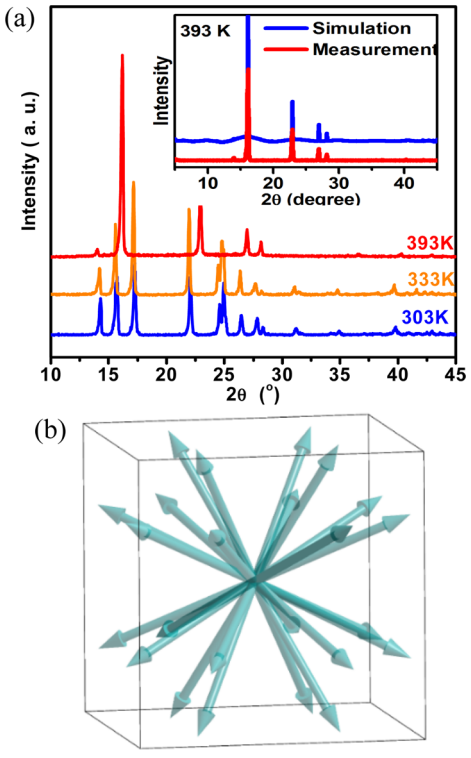

Figure 5. (a) The variable-temperature PXRD patterns of **1**. Inset: Pawley refinement of PXRD data of **1** collected at 393 K with a cubic unit cell of a = 10.9599 Å. (b) The schematic drawing of possible polarization vectors for the ferroelectric species of $m3mFm$(s).

(Figure 4e,f), which are typical evidence for the switching of ferroelectric domains. Moreover, the large amount of polarization directions can also be supported by local PFM study, which spontaneously recorded the in-plane and out-of-plane components of the piezoresponse, as shown in Figure S4, in the Supporting Information.

We have tried to determine the crystal structure of the PP to understand the ferroelectric origin and related phase-transition properties. Unfortunately, the single-crystal X-ray diffraction is too weak especially in range of the high 2θ angle to determine the structure. However, the good thermal stability up to 616 K (Figure S5) and reversibility do indicate that there is a stable PP. We then measured the variable-temperature PXRD (Figure 5). The patterns above T_c at 393 K show obvious changes in both the number and positions of the diffraction peaks. The diffraction characteristics remind us the plastic phase. The indexing of the PXRD pattern reveals a cubic lattice with a = 10.9599 Å. The Pawley refinements reveals a few possible cubic space groups, among which, the most possible space group is the $Fm3m$ if the LTP structure and the plastic feature are taken into account (inset of Figure 5). Thus, the HTP should have the well-known NaCl-type crystal structure, where the Na^+ and Cl^- ions are arranged alternatively along the three cell axes. As shown in Figure 2, such a structural character is unambiguous. We finally obtained the relationship of the two temperature cells: $\mathbf{a}^{LTP}$ (12.518(8) Å) ↔ $\mathbf{a}^{HTP}$ (10.9599 Å), $\mathbf{b}^{LTP}$ (7.417(4) Å) ↔ $-0.5\mathbf{b}^{HTP} + 0.5\mathbf{c}^{HTP}$ (7.7498 Å), $\mathbf{c}^{LTP}$ (c = 13.997(9) Å) ↔ $\mathbf{b}^{HTP} + \mathbf{c}^{HTP}$ (15.4996 Å), and that the ac plane of FP corresponds to the [0 1 1] plane of the PP (Figure 3). At this stage, one can qualitatively picture the structure of the PP as isostructural to the FCC NaCl.

With this model, the structural differences between the FP and PP become clear, and the ferroelectric mechanism can be accounted for. First, the main difference is in the order−disorder changes of the cations and anions. There are a few examples of solids with ball-like molecules that undergo plastic phase transitions before melting.[10] In this case, both the cation and the anion have the three-dimensional spherical geometry (Figure 1), which should contribute to the formation of the plastic phase as observed for other spherical molecules like tetramethylammonium, damantane and 1,4-diazabicyclo[2.2.2]-octane. In the HTP, both the cations and anions occupy the crystallographic special sites, and the high site symmetry is satisfied by their high orientational disorder. Second, there is an obvious relative shift along the low-temperature c-axis between two neighbored layers upon the transition. In the FCC structure of the HTP, the two neighbored layers along the a-axis are arranged in an eclipsed conformation so that the anion and cation are arrange alternatively and linearly along the a-axis. In the monoclinic structure of the FP, they are arranged in a staggered conformation (Figure 2a). The relative shift is as large as 3.5 Å, which usually cannot occur in the displacive-type phase transition. Such an unusual displacement contributes an insignificant polarization along the a-axis to the spontaneous polarization, because the shifted layers are neutral in charge. Third, there is an obvious relative displacement between the cations and anions in the same layer along the a-direction. This displacement is up to around 1.6 Å (Figure S6, Supporting Information). It can contribute directly to the spontaneous polarization. The exceptionally simple structure of **1** allows us to estimate their spontaneous polarization from the displacement of the ions. The calculated P_s is 8.39 $\mu C/cm^2$, very close to the experimental value (see the Supporting Information).

DOI: 10.1021/jacs.6b08817
J. Am. Chem. Soc. 2016, 138, 13175−13178

Because the FP has the space group *Cc*, the spontaneous polarization should be parallel to the *ac* plane. Correspondingly, the relative shift along the low-temperature *a*- and *c*-axes should be the origin of symmetry breaking and generation of ferroelectricity. The large displacements also indicate the high energy barrier of the phase transition, which results in the large thermal hysteresis (20 K) (Figure 3a), high latent heat and high E_c.

According to the Aizu rule, **1** belongs to the species of *m*3*m*F*m*(s) among the 88 species of ferroelectrics.[11] The FP and PP have 2 and 48 symmetry elements respectively, and thus there are 24 crystallographically equivalent polarization directions, corresponding to 12 ferroelectric axes, which are much more than the 3 ferroelectric axes of the widely used $BaTiO_3$ (Figure 5b).

In summary, we have discovered a molecular ferroelectric with 24 polarization directions, which is the most in known ferroelectrics. Such a large amount of equivalent polarizations in a ferroelectric compound predicts rich applications based on polarization switching and ferroelectric domain manipulation, especially in the form of polycrystalline phase. Because the multiple polarization direction is a direct result of the highly symmetric plastic phase, it is expected more multiaxial ferroelectrics can be designed by constructing crystals with spherical molecules and ions.

■ ASSOCIATED CONTENT

Supporting Information

The Supporting Information is available free of charge on the ACS Publications website at DOI: 10.1021/jacs.6b08817.

Data for $C_8H_{20}ClNO_4$ (CIF)
Experimental details (PDF)

■ AUTHOR INFORMATION

Corresponding Authors

*H.-Y.Y. hyye@seu.edu.cn
*Y.-M.Y. youyumeng@seu.edu.cn
*R.-G.X. xiongrg@seu.edu.cn

Notes

The authors declare no competing financial interest.

■ ACKNOWLEDGMENTS

This work was supported by 973 project (2014CB932103) and the National Natural Science Foundation of China (21290172, 91222101, 21371032 and 21573041).

■ REFERENCES

(1) (a) Horiuchi, S.; Tokura, Y. *Nat. Mater.* **2008**, *7*, 357. (b) Liao, W. Q.; Zhang, Y.; Hu, C. L.; Mao, J. G.; Ye, H.-Y.; Li, P. F.; Huang, S. D.; Xiong, R.-G. *Nat. Commun.* **2015**, *6*, 7338. (c) Ye, H.-Y.; Zhou, Q.; Niu, X.; Liao, W.-Q.; Fu, D.-W.; Zhang, Y.; You, Y.-M.; Wang, J.; Chen, Z.-N.; Xiong, R.-G. *J. Am. Chem. Soc.* **2015**, *137*, 13148. (d) Zhang, Y.; Liao, W. Q.; Fu, D. W.; Ye, H.-Y.; Chen, Z. N.; Xiong, R.-G. *J. Am. Chem. Soc.* **2015**, *137*, 4928. (e) Xu, G. C.; Zhang, W.; Ma, X. M.; Chen, Y. H.; Zhang, L.; Cai, H. L.; Wang, Z. M.; Xiong, R.-G.; Gao, S. *J. Am. Chem. Soc.* **2011**, *133*, 14948. (f) Di Sante, D.; Stroppa, A.; Jain, P.; Picozzi, S. *J. Am. Chem. Soc.* **2013**, *135*, 18126. (g) Akutagawa, T.; Koshinaka, H.; Sato, D.; Takeda, S.; Noro, S.; Takahashi, H.; Kumai, R.; Tokura, Y.; Nakamura, T. *Nat. Mater.* **2009**, *8*, 342. (h) Zhang, W.; Xiong, R.-G. *Chem. Rev.* **2012**, *112*, 1163. (i) Tian, Y.; Shen, S.; Cong, J.; Yan, L.; Wang, S.; Sun, Y. *J. Am. Chem. Soc.* **2016**, *138*, 782. (j) For more literatures about molecular ferroelectrics, see ref S2 in the Supporting Information.

(2) Stroppa, A.; Di Sante, D.; Barone, P.; Bokdam, M.; Kresse, G.; Franchini, C.; Whangbo, M. H.; Picozzi, S. *Nat. Commun.* **2014**, *5*, 5900.

(3) (a) Katrusiak, A.; Szafranski, M. *Phys. Rev. Lett.* **1999**, *82*, 576. (b) Szafranski, M.; Katrusiak, A.; McIntyre, G. J. *Phys. Rev. Lett.* **2002**, *89*, 215507. (c) Harada, J.; Shimojo, T.; Oyamaguchi, H.; Hasegawa, H.; Takahashi, Y.; Satomi, K.; Suzuki, Y.; Kawamata, J.; Inabe, T. *Nat. Chem.* **2016**, *8*, 946.

(4) (a) Sun, Z.; Chen, T.; Liu, X.; Hong, M.; Luo, J. *J. Am. Chem. Soc.* **2015**, *137*, 15660. (b) Horike, S.; Umeyama, D.; Inukai, M.; Itakura, T.; Kitagawa, S. *J. Am. Chem. Soc.* **2012**, *134*, 7612. (c) Wang, P.; Dai, Q.; Zakeeruddin, S. M.; Forsyth, M.; MacFarlane, D. R.; Gratzel, M. *J. Am. Chem. Soc.* **2004**, *126*, 13590.

(5) Kivikoski, J.; Howard, J. A. K.; Kelly, P.; Parker, D. *Acta Crystallogr., Sect. C: Cryst. Struct. Commun.* **1995**, *51*, 535.

(6) Fukunaga, M.; Noda, Y. *J. Phys. Soc. Jpn.* **2008**, *77*, 064706.

(7) (a) Fu, D. W.; Cai, H. L.; Liu, Y. M.; Ye, Q.; Zhang, W.; Zhang, Y.; Chen, X. Y.; Giovannetti, G.; Capone, M.; Li, J. Y.; Xiong, R.-G. *Science* **2013**, *339*, 425. (b) Fu, D. W.; Zhang, W.; Cai, H. L.; Zhang, Y.; Ge, J. Z.; Xiong, R.-G.; Huang, S. D. *J. Am. Chem. Soc.* **2011**, *133*, 12780. (c) Ye, H.-Y.; Li, S. H.; Zhang, Y.; Zhou, L.; Deng, F.; Xiong, R.-G. *J. Am. Chem. Soc.* **2014**, *136*, 10033. (d) Horiuchi, S.; Kagawa, F.; Hatahara, K.; Kobayashi, K.; Kumai, R.; Murakami, Y.; Tokura, Y. *Nat. Commun.* **2012**, *3*, 1308. (e) Tayi, A. S.; Kaeser, A.; Matsumoto, M.; Aida, T.; Stupp, S. I. *Nat. Chem.* **2015**, *7*, 281.

(8) Horiuchi, S.; Tokunaga, Y.; Giovannetti, G.; Picozzi, S.; Itoh, H.; Shimano, R.; Kumai, R.; Tokura, Y. *Nature* **2010**, *463*, 789.

(9) (a) Balke, N.; Bdikin, I.; Kalinin, S. V.; Kholkin, A. L. *J. Am. Ceram. Soc.* **2009**, *92*, 1629. (b) Kalinin, S. V.; Bonnell, D. A. *Phys. Rev. B: Condens. Matter Mater. Phys.* **2002**, *65*, 125408. (c) Lu, H.; Bark, C. W.; de los Ojos, D. E.; Alcala, J.; Eom, C. B.; Catalan, G.; Gruverman, A. *Science* **2012**, *336*, 59.

(10) (a) Folmer, J. C. W.; Withers, R. L.; Welberry, T. R.; Martin, J. D. *Phys. Rev. B: Condens. Matter Mater. Phys.* **2008**, *77*, 144205. (b) Sato, K.; Iwai, M.; Sano, H.; Konno, M. *Bull. Chem. Soc. Jpn.* **1984**, *57*, 634.

(11) Aizu, K. *J. Phys. Soc. Jpn.* **1969**, *27*, 387.

DOI: 10.1021/jacs.6b08817
J. Am. Chem. Soc. 2016, 138, 13175−13178